JOURNAL OF MATERIALS SCIENCE **33** (1998) 4747–4758

Phase-transformation study of metastable tetragonal zirconia powder

NAOKI IGAWA, TAKANORI NAGASAKI*, YOSHINOBU ISHII, KENJI NODA, HIDEO OHNO, YUKIO MORII
Japan Atomic Energy Research Institute, Tokai-mura, Ibaraki-ken, 319-1195, Japan
E-mail: igawa@maico.tokai.jaeri.go.jp

JAIME A. FERNANDEZ-BACA
Oak Ridge National Laboratory, Oak Ridge, TN 37831-6393, USA

The rate of the transformation from the metastable tetragonal to the monoclinic phase of ZrO_2 was measured in air from 850 °C to 1000 °C by neutron diffraction. This rate was found to be temperature dependent, and its measured values were considerably lower then those reported previously. The kinetics of this phase transformation is discussed in terms of a modified 'crystallite growth-martensitic transformation model' that includes the distribution of crystallite sizes.

1. Introduction

It is well known that stabilized tetragonal zirconia has high strength and toughness properties [1]. The reason for these qualities is generally believed to be that the tetragonal phase martensitically transforms to the monoclinic phase—due to the applied stress [2] in a process that is not based on the thermal activation. There are, however, several experimental reports that suggest that this transformation can also depend on the thermally activated process. The tetragonal-to-monoclinic transformation of the PSZ(partially stabilized zirconia) at relatively low temperature annealing [3] and the phase transformation of the metastable tetragonal zirconia [4–5] are two examples of this.

Only a few studies of the kinetics of the transformation of the metastable tetragonal to the monoclinic phase of pure ZrO_2 have been reported. Whitney [4] measured the isothermal transformation rate of the metastable tetragonal to monoclinic ZrO_2 by X-ray diffraction using a sample prepared from zirconyl chloride octahydrate by thermal decomposition. Ohno *et al*. [5] carried out similar experiments using both neutron and X-ray diffraction. These reports showed that the transformation rate increased with temperature according to Avrami's rate equation [6], which is based on the nucleation and growth of a new phase.

On the other hand, Murakami and Ohno [7] investigated the effect of the crystallite size and the annealing temperature on the phase transformation and pointed out that the phase transformation was closely related to the growth of the crystallite size. They supported the idea of the 'critical diameter (crystallite size)' proposed by Garvie [8], in which the tetragonal crystallites grow during annealing, and transform immediately to the monoclinic phase upon reaching a critical diameter. In this process the transformation rate is not caused by the nucleation and growth of a new phase(Avrami's model) but by the growth of existing crystallites beyond this critical diameter. Murakami and Ohno called this model the 'crystallite growth–martensitic transformation model.'

In this paper, we combine this model with the distribution of the crystallite size and the normal grain-growth mechanism to develop and formulate a more quantitative model of the 'crystallite growth–martensitic transformation model.' To test our model, we carried out a neutron-diffraction study of the transformation rate of a highly homogenous sample of metastable tetragonal ZrO_2 prepared by the alkoxide method.

2. Experimental procedure

The metastable tetragonal zirconia powder was obtained from zirconium tetra-*n*-butoxide (99.9%, $Zr(OC_4H_9)_4$, Soekawa Chemicals Co. Ltd., Japan) by the alkoxide method. Details of the preparation of the metastable tetragonal zirconia powder were described elsewhere [9]. Although the sample was amorphous after drying, a single phase of the metastable tetragonal phase appeared immediately by heating at 400 °C in air. To remove any organic impurities derived from the thermal decomposition on n-C_4H_9OH, we annealed the sample at about 700 °C for 10 min in air. Secondary particles were almost spheres with nearly the same size, and their mean particle size was 0.55 μm observed with a scanning-electron microscope(SEM). The mean

*Now at Nagoya University, Chikusa-ku, Nagoya-shi, 464-01, Japan.

crystallite size was 16 nm calculated from the (1 0 1) peak of X-ray diffraction using the Scherrer formula:

$$D = \frac{0.9\lambda}{\beta \cos\theta} \quad (1)$$

where D is the crystallite size, λ the wavelength of X-ray, β the corrected half-width of diffraction peak and θ the diffraction-peak angle respectively.

Neutron-diffraction experiments were performed using the Wide Angle Neutron Diffractometer (WAND) at Oak Ridge National Laboratory (ORNL), USA. A wavelength of 0.1537 nm was used in this experiment. The detector of the WAND is a curved one-dimensional position-sensitive proportional counter which covers a 2θ range from about 10° to 140°. The sample was annealed in air in the temperature range from 850 °C to 1000 °C using a rapid temperature change furnace [10] equipped at the WAND. We placed a platinum sample holder of 3 mm in dia and 30 mm in height at the focal points of two circular infrared lamps inside the furnace. The temperature was controlled within ±5 °C with a type-K thermocouple inserted within the sample with the temperature difference between the surface of the sample holder and the center of the sample being less than 10 °C. The heating rate was 200 °C/min. Since more than a few minutes were needed to collect peak counts with meaningful statistics to determine the ratio between the tetragonal and monoclinic phases, we quenched the sample to 100 °C at the rate of about −200 °C/min after annealing. The transformation rate of the tetragonal to the monoclinic phase was measured at 100 °C because the transformation rate is negligible below this temperature. The measurement time was about 30 min. After measuring the phase transformation ratio, we heated the sample again to the annealing temperature. We defined the starting time, $t = 0$ as the time that the temperature first reaches the annealing temperature. The overall annealing time referred to in this paper is the total time the sample was at the annealing temperature, and does not include the heating and cooling time.

We determined the molar fraction of the monoclinic phase, F_M and the metastable tetragonal phase, F_T by the intensity relationship:

$$F_M = \frac{I_M(1\,1\,1) + I_M(1\,1\,\bar{1})}{I_M(1\,1\,1) + I_T(1\,0\,1) + I_M(1\,1\,1)} \quad (2)$$

and

$$F_T = 1 - F_M \quad (3)$$

where $I_M(1\,1\,1)$, $I_M(1\,1\,\bar{1})$ and $I_T(1\,0\,1)$ are the peak intensities of the (1 1 1) and (1 1 1) reflections of the monoclinic phase and the (1 0 1) reflection of the metastable tetragonal phase respectively. To confirm the linearity of Equation 2, we made standard samples which were mixtures of pure-metastable tetragonal ZrO_2 and pure-monoclinic ZrO_2 powders. Fig. 1 shows F_M as a function of the molar fraction of the samples. It is apparent that F_M is proportional to the mol % of the monoclinic phase.

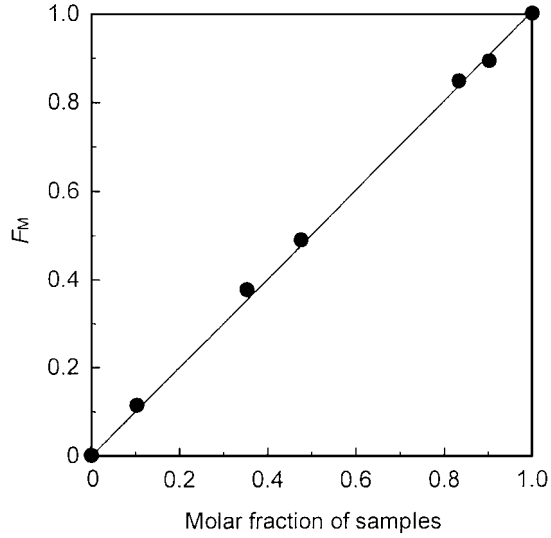

Figure 1 Calibration plots of F_M, the relative content of the monoclinic ZrO_2.

3. Results and discussion

3.1. The transformation rates of the metastable tetragonal ZrO_2 to the monoclinic phase

Fig. 2 shows the details of the analysis of the deconvolution of three peaks, the (1 1 1) and (111) of the monoclinic phase and the (1 0 1) of the tetragonal phase, at 875 °C. The tetragonal peak decreased gradually by increasing the annealing time and almost disappeared after 2000 min. Fig. 3 shows the time dependence of the transformed fraction, $F_M(t)$ at the temperature range 850 °C to 1000 °C. The symbols indicate the observed data, while the solid lines are guides to the eye. The phase-transformation rate increases by increasing the annealing temperature. At 1000 °C the phase transformation ended within 100 min while it took more than 4000 min to complete at 850 °C. The transformation rates in the present work are considerably lower than those reported by Whitney and Ohno et al. For example, the phase transformation completed within a few hours even at 650 °C in Whitney's result. Although the transformation rates of Ohno's X-ray and neutron diffraction were very different (Fig. 4), the phase transformation ended within 2000 min at 750 °C.

3.2. Modeling of the phase transformation of the metastable tetragonal ZrO_2 and fitting the present work

To discuss the phase-transformation kinetics, we formulate the phase transformation using the 'crystallite growth–martensitic transformation model'; the tetragonal zirconia has a critical diameter, and the crystallites which grow to exceed this value martensitically transform to the monoclinic phase. We now proceed to describe a set of four postulates.

Postulate 1: Critical diameter: Zirconia has a critical diameter. The monoclinic phase is stable for crystallites of sizes above this value, while the tetragonal phase is stable for crystallites of sizes below it [8].

Postulate 2: Martensitic transformation: When the diameter of a crystallite exceeds the critical value, the

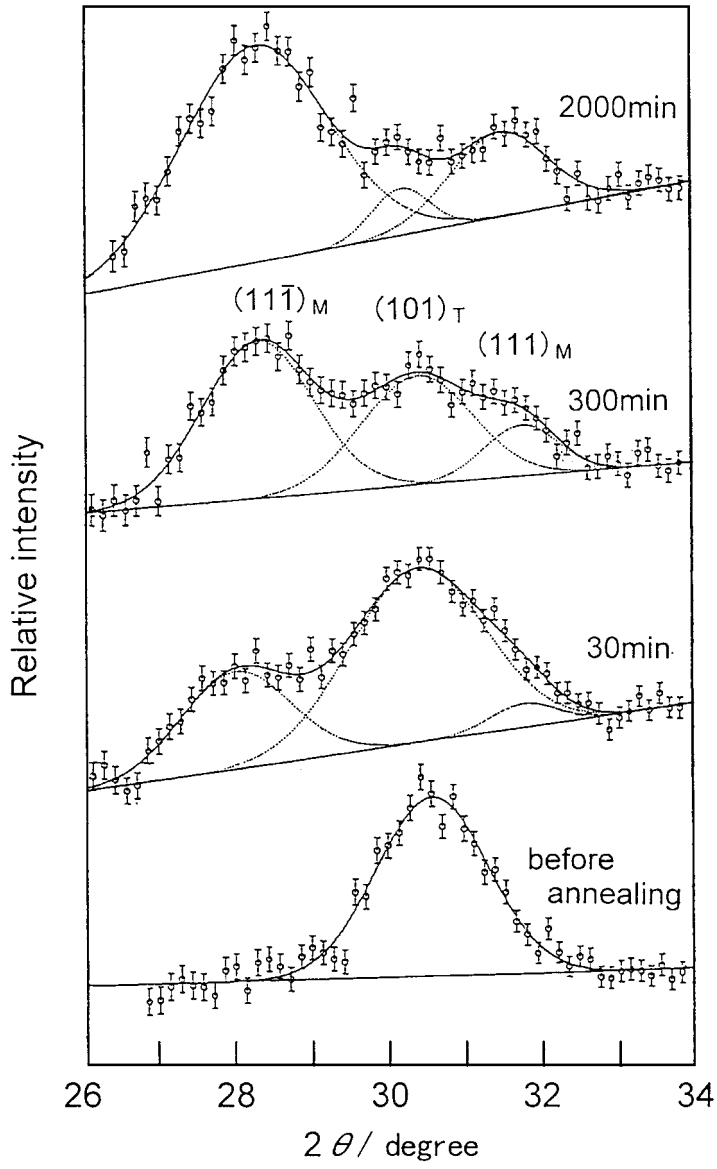

Figure 2 Typical results of deconvolution of diffraction patterns to the (1 0 1) of the tetragonal and the (1 1 1) and (1 1 $\bar{1}$) of the monoclinic phase at different times at 875 °C.

crystallite is immediately transformed from the tetragonal to the monoclinic phase [8].

Postulate 3: Normal crystallite growth: The crystallite growth of an individual tetragonal crystallite at a constant temperature is characterized by

$$d(t)^n - d(0)^n = K_n t \tag{4}$$

where $d(t)$ is the metastable tetragonal crystallite size at time t, and $d(0)$ is the initial crystallite size [11] before annealing. The exponent n is a constant depending on the mechanism of the crystallite growth, and K_n is a constant, which contains the temperature dependence of grain growth.

We introduce the normalized crystallite size, L to simplify the calculation. We define

$$L \equiv \frac{d}{d_p} \tag{5}$$

and

$$D \equiv \ln L. \tag{6}$$

where d_p is the most probable value of d.

Postulate 4: Time-independent log-normal distribution: The metastable tetragonal crystallite diameter has a log-normal distribution [12].

Thus the probability, $G(D)\mathrm{d}D$, that D falls between D and $D + \mathrm{d}D$ is given by

$$G(D)dD \propto \exp\left[-\frac{(D - D_{av})^2}{2\sigma^2}\right]dD$$
$$= \exp\left[-\frac{(D - D_p)^2}{2\sigma^2}\right]dD = \exp\left(-\frac{D^2}{2\sigma^2}\right)dD, \tag{7}$$

where σ is the standard deviation. In the metal field, several reports suggested that σ is constant during the crystallite growth [12, 13]. Therefore we assumed that

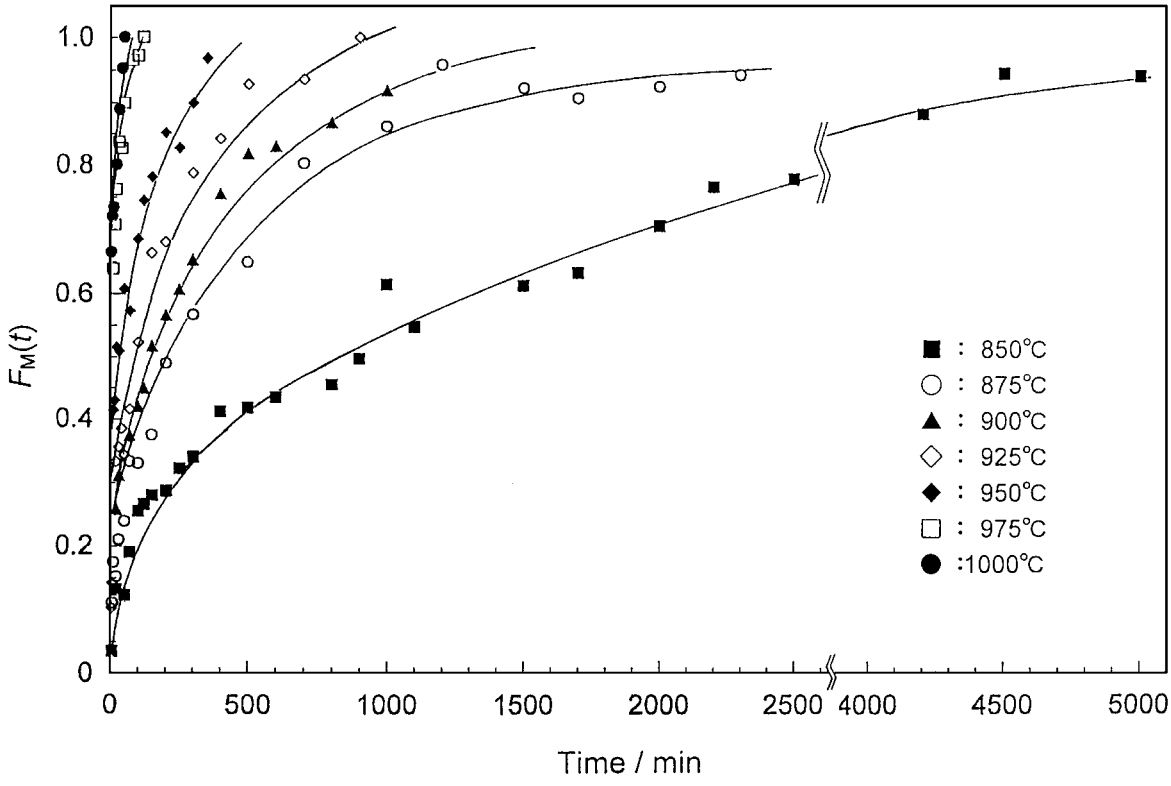

Figure 3 Time dependence of $F_M(t)$, the transformed fraction at the temperatures ranging from 850 °C to 1000 °C. The symbols indicate the observed data. The solid lines are the guide to the eye.

σ is constant throughout the crystallite growth in this study.

The probability, $g(L)\mathrm{d}L$, that L falls between L and $L + \mathrm{d}L$ is given by

$$g(L)dL = G(D)LdD \propto \exp\left(D - \frac{D^2}{2\sigma^2}\right)dD. \quad (8)$$

If all the sample has a tetragonal phase, the molar fraction, F of crystallites smaller than a diameter, d is given by

$$F = \frac{\int_0^D \rho L^3 g(L)dL}{\int_0^\infty \rho L^3 g(L)dL}, \quad (9)$$

where D is the same as in Equation 6, and ρ is the density of the metastable tetragonal phase.

The crystallites of sizes greater then a critical diameter, d_c transform to the monoclinic phase with a volume change. The molar fraction of the remaining metastable tetragonal phase in Equation 9 is given by

$$F_T = \frac{\int_0^{D_c} \rho L^3 g(L)dL}{\int_0^{D_c} \rho L^3 g(L)\,dL + \int_{D_c}^\infty \rho_M L_M^3 g(L_M)\,dL_M}, \quad (10)$$

where $L_M = d_M/d_p$, ρ_M is the density of the monoclinic phase. The relationship between the diameter of the monoclinic phase, d_M and d before phase transformation is

$$\rho_M d_M^3 = \rho d^3. \quad (11)$$

Since the probability, $g(L_M)\mathrm{d}L_M$, that L_M falls between L_M and $L_M + \mathrm{d}L_M$ is equal to $g(L)\,dL$, Equation 10 is rewritten

$$\begin{aligned} F_T &= \frac{\int_0^{D_c} \rho L^3 g(L)\,dL}{\int_0^{D_c} \rho L^3 g(L)\,dL + \int_{D_c}^\infty \rho L^3 g(L)\,dL} \\ &= \frac{\int_0^{D_c} \rho L^3 g(L)dL}{\int_0^\infty \rho L^3 g(L)dL} = \frac{\int_{-\infty}^{D_c} e^{4D} G(D)dD}{\int_{-\infty}^\infty e^{4D} G(D)dD} \\ &= \left[\int_{-\infty}^{D_c} \exp\left(4D - \frac{D^2}{2\sigma^2}\right)dD\right] \Big/ \\ &\quad \left[\int_{-\infty}^\infty \exp\left(4D - \frac{D^2}{2\sigma^2}\right)dD\right], \end{aligned} \quad (12)$$

where $D_c = \ln(d_c/d_p)$.

If we make the transformation

$$D' = \frac{D}{\sigma} - 4\sigma, \quad (13)$$

Equation 12 becomes

$$\begin{aligned} F_T &= \left[\sigma e^{8\sigma^2} \int_{-\infty}^{D_c'} \exp\left(-\frac{D'^2}{2}\right)dD'\right] \Big/ \\ &\quad \left[\sigma e^{8\sigma^2} \int_{-\infty}^\infty \exp\left(-\frac{D'^2}{2}\right)dD'\right] \\ &= \frac{1}{(2\pi)^{1/2}} \int_{-\infty}^{D_c'} \exp\left(-\frac{D'^2}{2}\right)dD', \end{aligned} \quad (14)$$

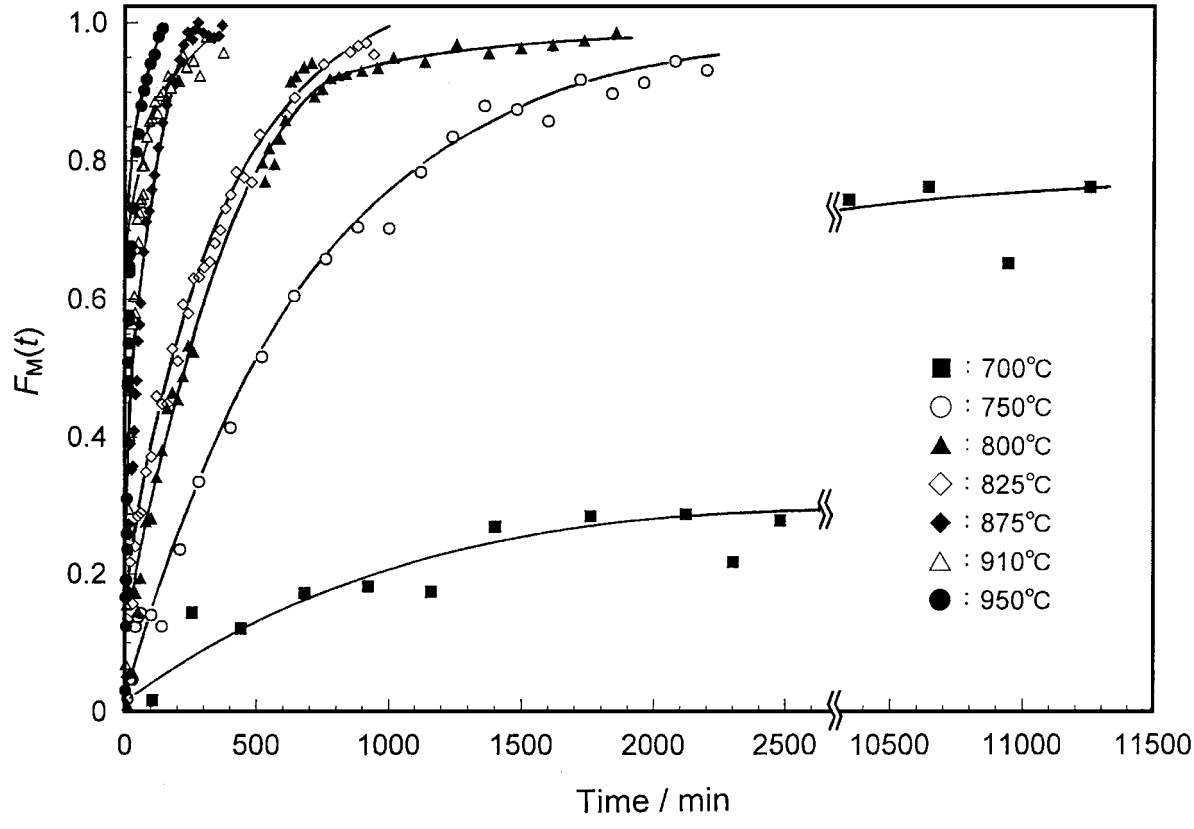

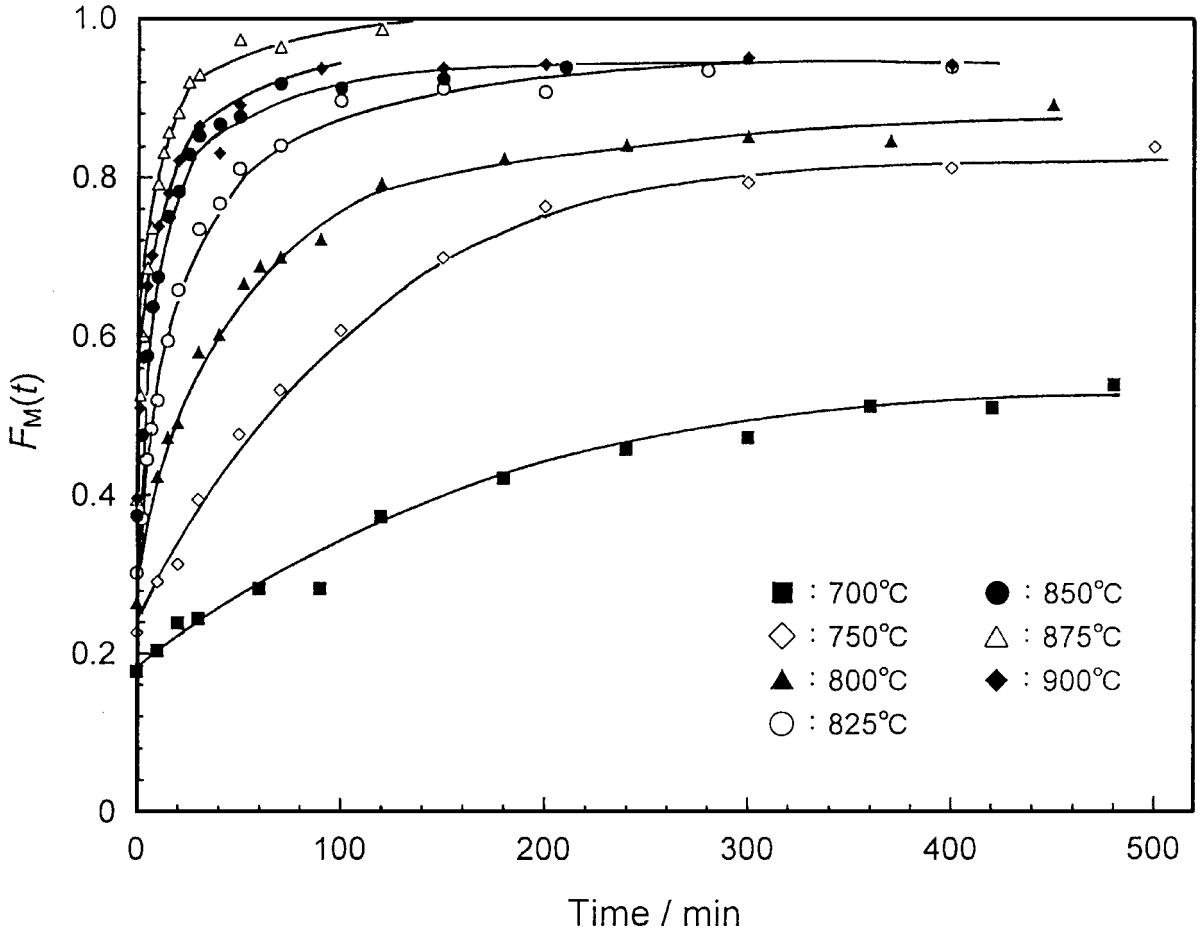

Figure 4 Time dependence of $F_M(t)$ in Ohno's experiment: (a) neutron diffraction, (b) X-ray diffraction.

where

$$D'_c = \frac{D_c}{\sigma} - 4\sigma. \tag{15}$$

If the mean crystallite size changes following the relationship,

$$d_m(t)^n - d_m(0)^n = K_n t \tag{16}$$

or

$$\frac{d_m(t)}{d_m(0)} = \sqrt[n]{1 + \frac{K_n t}{d_m(0)^n}}, \tag{17}$$

we can estimate $F_M(= 1 - F_T)$ at time t from Equations 14 and 17.

Since we defined L_m as

$$\frac{d_m}{d_p} = L_m = \int_0^\infty Lg(L)dL = e^{2\sigma^2}, \tag{18}$$

d_m/d_p is independent of t.

From the Postulate 4, σ is independent of t, thus Equation 17 can be rewritten as

$$\frac{d_p(t)}{d_p(0)} = \sqrt[n]{1 + \frac{K_n t}{d_p(0)^n}} \equiv \sqrt[n]{1 + \frac{t}{\tau_n}}. \tag{19}$$

Since $L_c(t)$ can be rewritten as

$$L_c(t) = \frac{d_c}{d_p(t)} = \frac{d_c}{d_p(0)} \frac{d_p(0)}{d_p(t)}, \tag{20}$$

we get

$$D_c(t) = \ln\frac{d_c}{d_p(0)} - \ln\frac{d_p(t)}{d_p(0)} = D_c(0) - \frac{1}{n}\ln\left(1 + \frac{t}{\tau_n}\right). \tag{21}$$

Substituting D_c from Equation 13 into Equation 21, we have

$$D'_c(t) = \ln\frac{D_c(t)}{\sigma} - 4\sigma = D'_c(0) - \frac{1}{n\sigma}\ln\left(1 + \frac{t}{\tau_n}\right) \tag{22}$$

where

$$D'_c(0) = \frac{D_c(0)}{\sigma} - 4\sigma. \tag{23}$$

Thus calculating the $D'_c(t)$ from the observed F_M, we can obtain $D'_c(0)$, $n\sigma$ and τ_n by a non-linear least-squares fit.

When F_M was measured at temperatures T lower than the annealing temperature, we chose the critical diameter at T, $d_{c,T}$ instead of the critical diameter at the annealing temperature, d_c; although the tetragonal phase is stable in the crystallite whose diameter is between $d_{c,T}$ and d_c at the annealing temperature [7], the tetragonal phase transforms to the monoclinic phase in these crystallites during cooling.

Since we measured F_M at 100 °C after annealing, $D_c(t)$ in Equation 21 is expressed as

$$D_c(t) = \ln\frac{d_{c,100}}{d_p(0)} - \ln\frac{d_p(t)}{d_p(0)} = D_{c,100}(0) - \frac{1}{n}\ln\left(1 + \frac{t}{\tau_n}\right), \tag{24}$$

where $d_{c,100}$ is the critical diameter at 100 °C.

Substituting D_c from Equation 13 into Equation 24, we have

$$D'_c(t) = \ln\frac{D_{c,100}(t)}{\sigma} - 4\sigma = D'_{c,100}(0) - \frac{1}{n\sigma}\left(1 + \frac{t}{\tau_n}\right), \tag{25}$$

where

$$D'_{c,100}(0) = \frac{D_{c,100}(0)}{\sigma} - 4\sigma. \tag{26}$$

Comparing Equation 22 with Equation 25, we can establish that $n\sigma$ and τ_n measured at the annealing temperature are the same as those measured at 100 °C.

Figs 5–6 show the result of fitting our data to Equation 25. We can not fit the data well if we allow n to vary with the annealing temperature. Thus we assume that n is independent of the annealing temperature in the present temperature range. The symbols indicate the observed data, while solid lines are the results of the least-squares fitting. The fits to Equation 25 shown in Fig. 5 are rather good for all temperatures except for 1000 °C. The reason for the discrepancy at 1000 °C is probably that in our analysis we did not consider the effects of the heating and cooling time. The obtained least-square fit parameters are listed in Table I. $D'_{c,100}(0)$ decreases with increasing the annealing temperature systematically. As shown in Equations 24 and 26, $d_p(0)$ increases with the annealing temperature because $d_{c,100}$ is independent of the annealing temperature. The reason for this is that the crystallite size at $t = 0$ increases with the annealing temperature; the crystallite grew until the temperature first reached the annealing temperature. τ_n also decreases with increasing the annealing temperature. Since $d_p(0)$ increases with the annealing temperature, while we assumed that n does not, this indicates that K_n also increases with the annealing temperature.

TABLE I Least square fit result of the present work

$n\sigma = 1.22 \pm 0.08$

Temperature	$D'_{c,100}(0)$	τ_n
850 °C	1.23 ± 0.09	218.3 ± 52.6
875 °C	1.16 ± 0.10	68.6 ± 18.8
900 °C	0.85 ± 0.15	75.3 ± 23.7
925 °C	1.12 ± 0.11	28.5 ± 7.8
950 °C	0.42 ± 0.13	40.7 ± 11.9
975 °C	0.53 ± 0.52	5.6 ± 4.5
1000 °C	-0.24 ± 0.17	11.7 ± 4.5

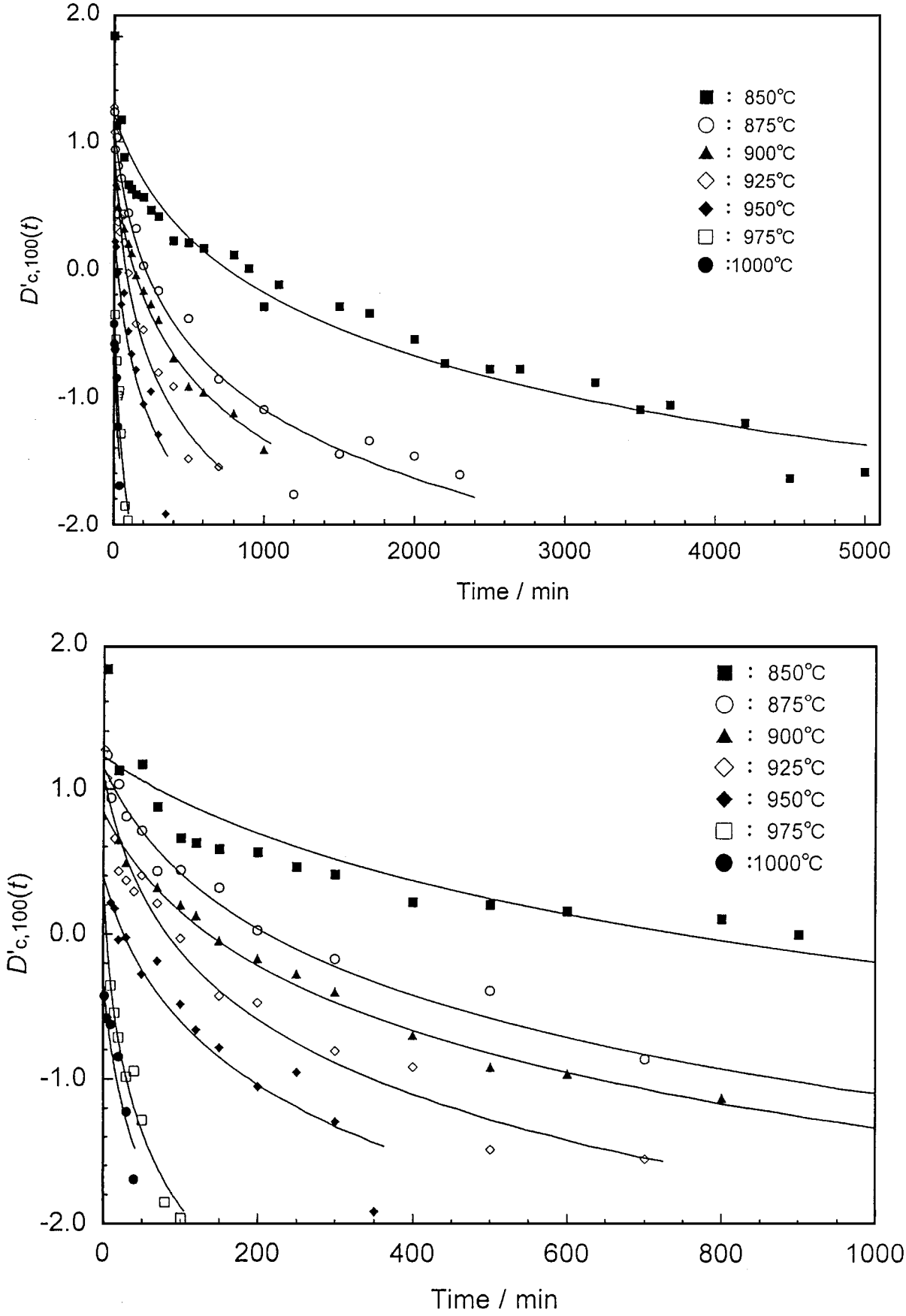

Figure 5 The least-squares fits of $D'_{c,100}(t)$ of the present work as a function of $D'_{c,100}(0)$, $n\sigma$ and τ_n by Equation 21: (a) time range from 0 to 5000 min, (b) time range from 0 to 1000 min. The symbols indicate the observed data, and the solid lines are the fitted curves.

3.3. Fitting previous results to the present model

We also fitted Ohno's X-ray and neutron diffraction data to our model although the quantitative agreement between Ohno's X-ray and neutron experiments is poor. Since they measured F_M at the annealing temperature, we fitted Ohno's neutron and X-ray diffraction data to Equation 22. We assumed that n is independent of the

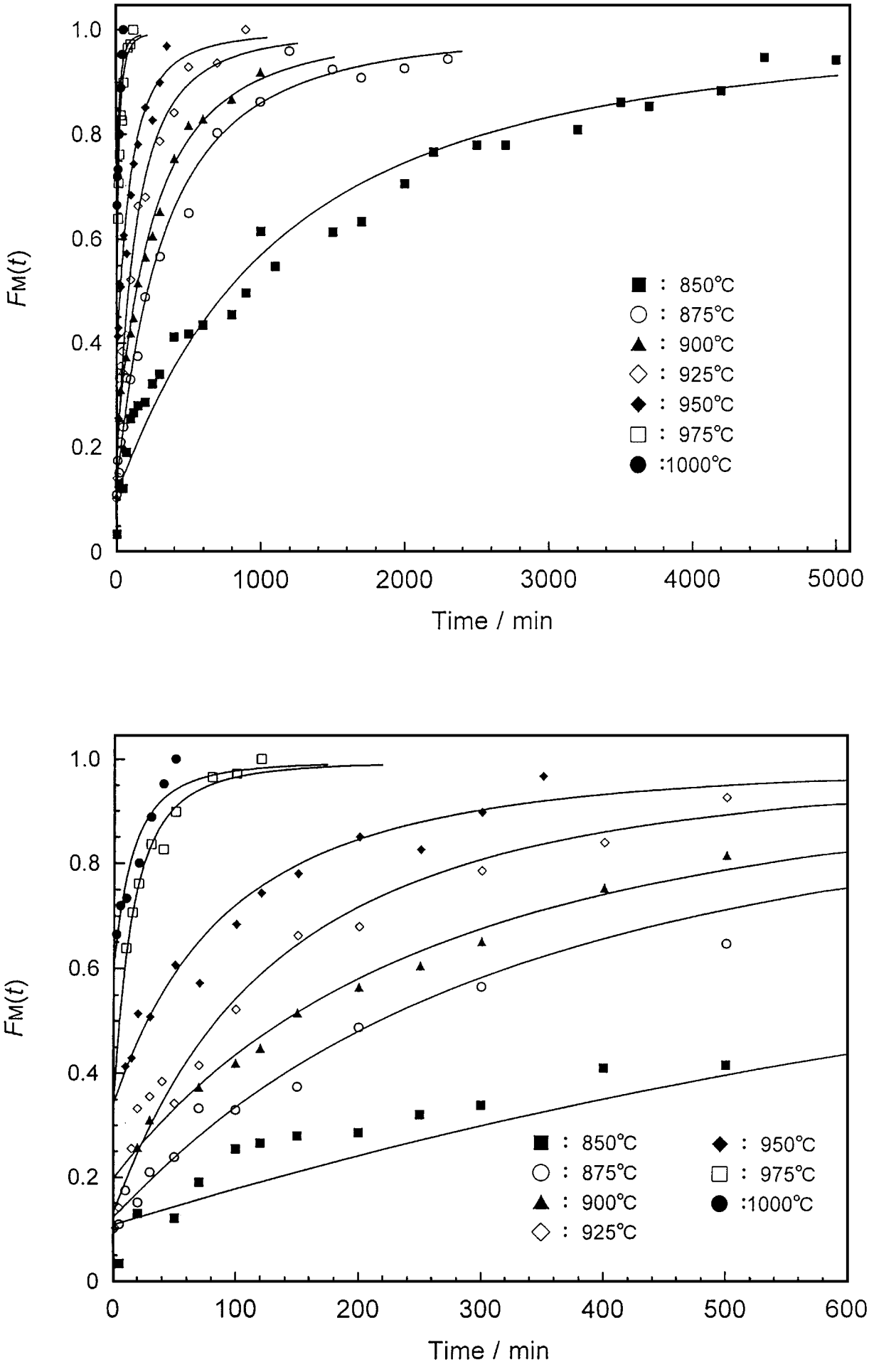

Figure 6 The results of $F_M(t)$ of the present work as a function of $D'_{c,100}(0)$, $n\sigma$ and τ_n by Equation 21: (a) time range from 0 to 5000 min, (b) time range from 0 to 600 min.

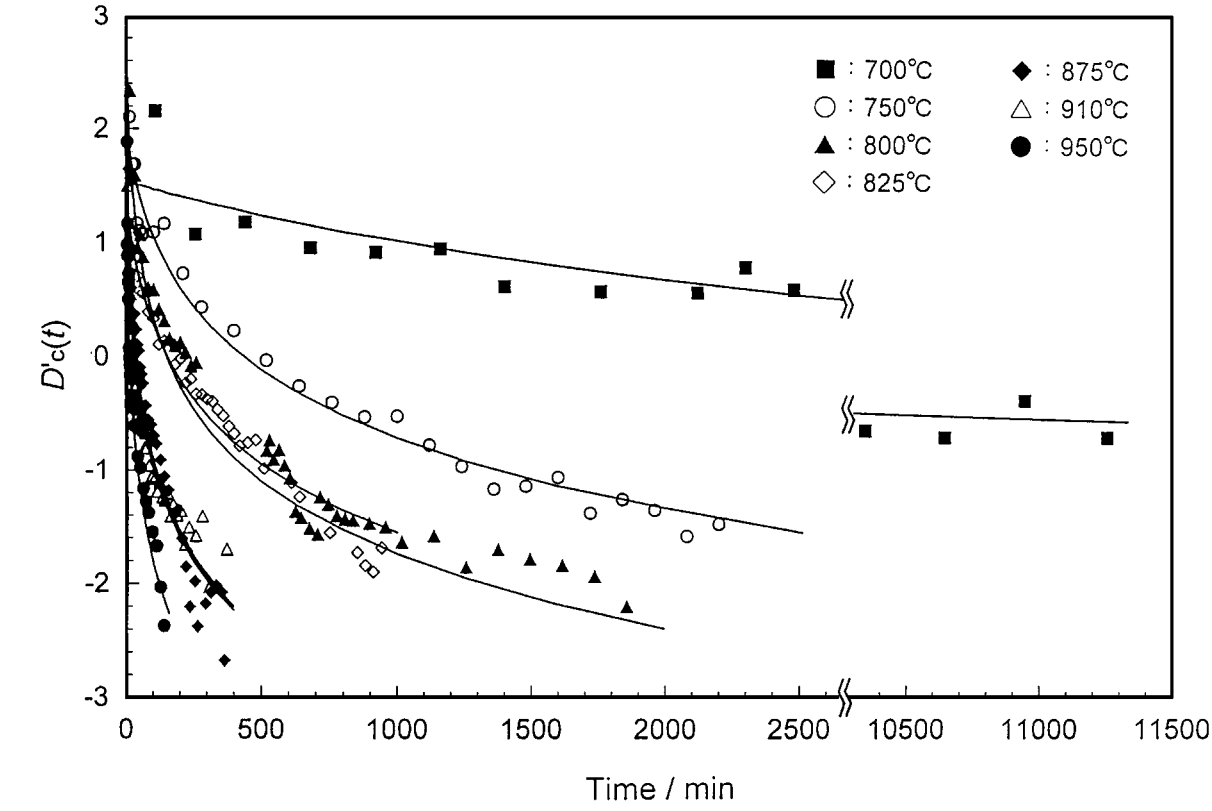

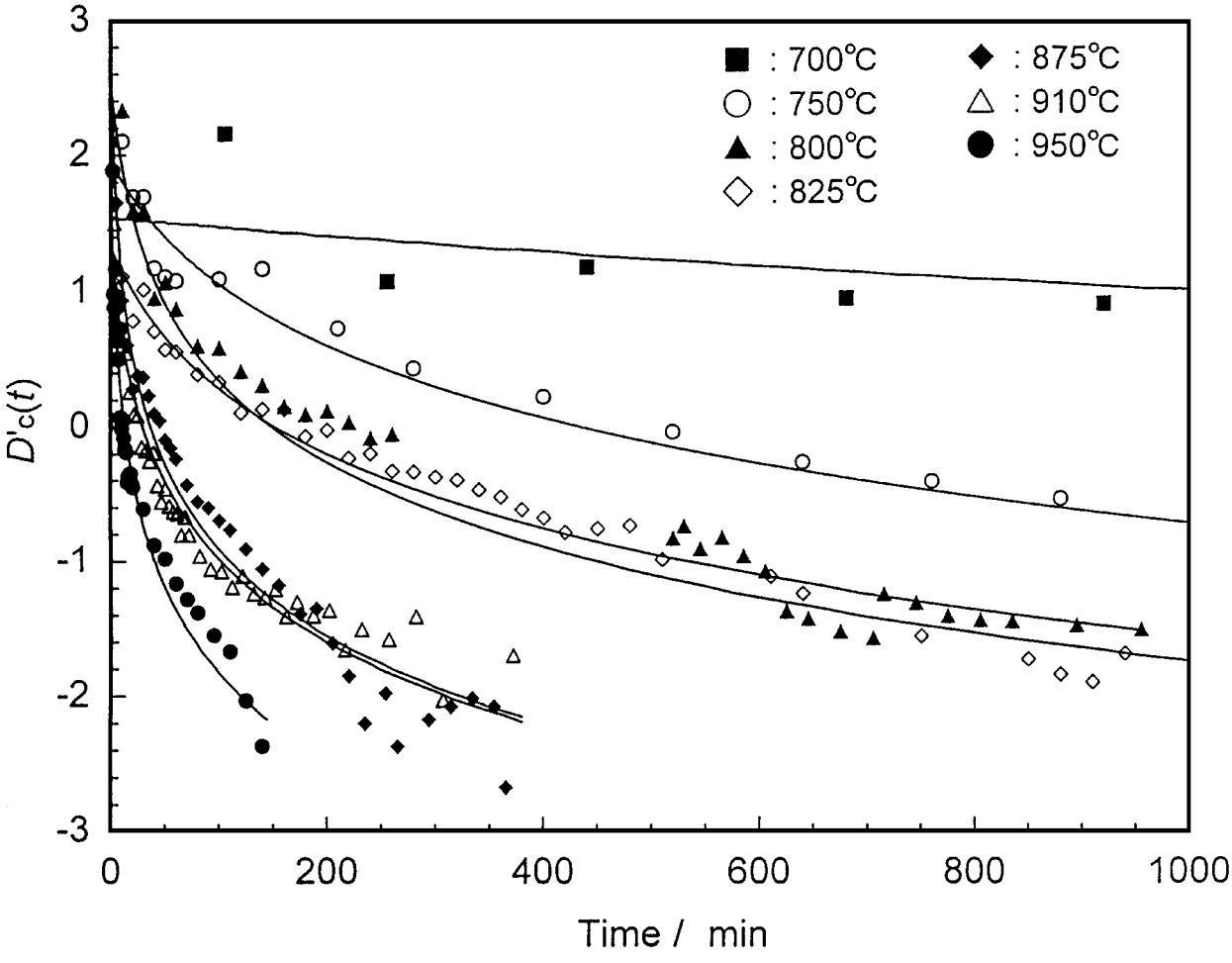

Figure 7 The results of $D'_c(t)$ of Ohno's neutron diffraction as a function of $D'_c(0)$, $n\sigma$ and τ_n by Equation 18: (a) time range from 0 to 11500 min, (b) time range from 0 to 1000 min.

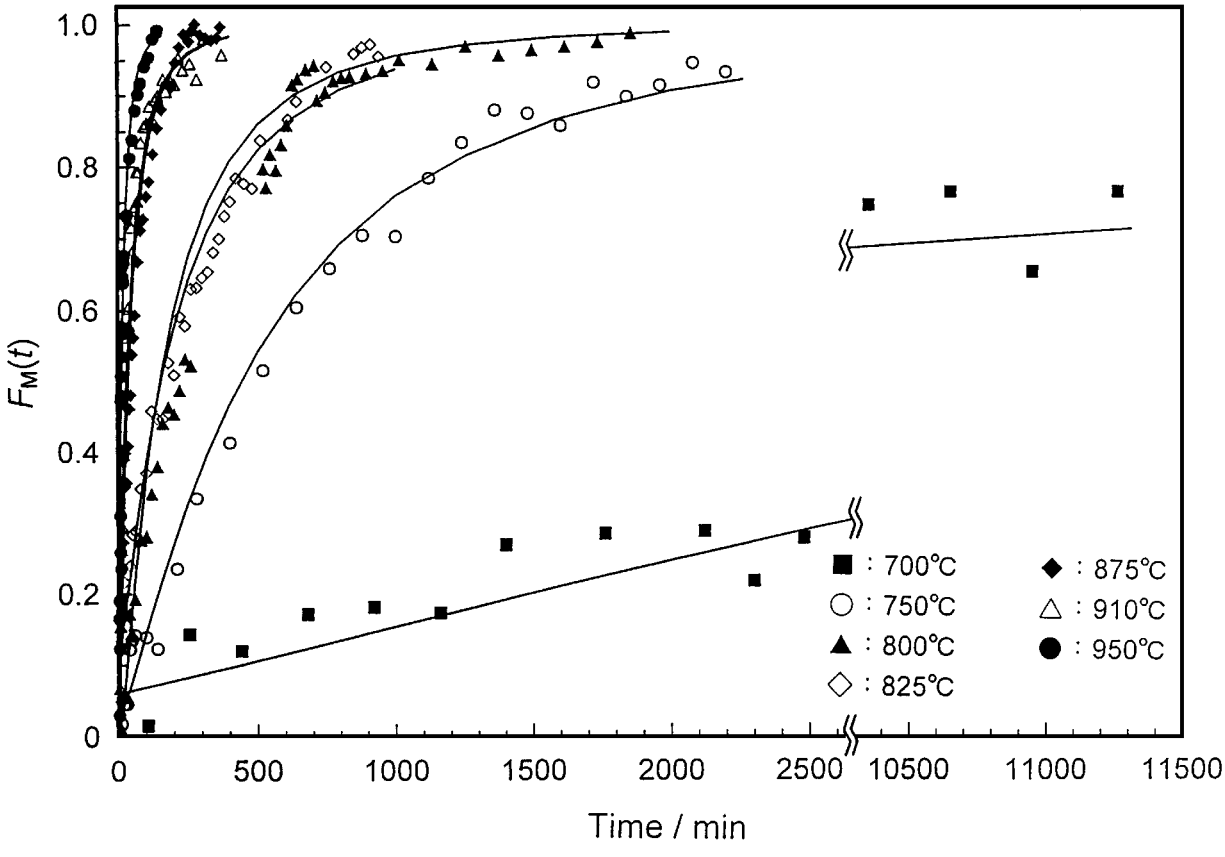

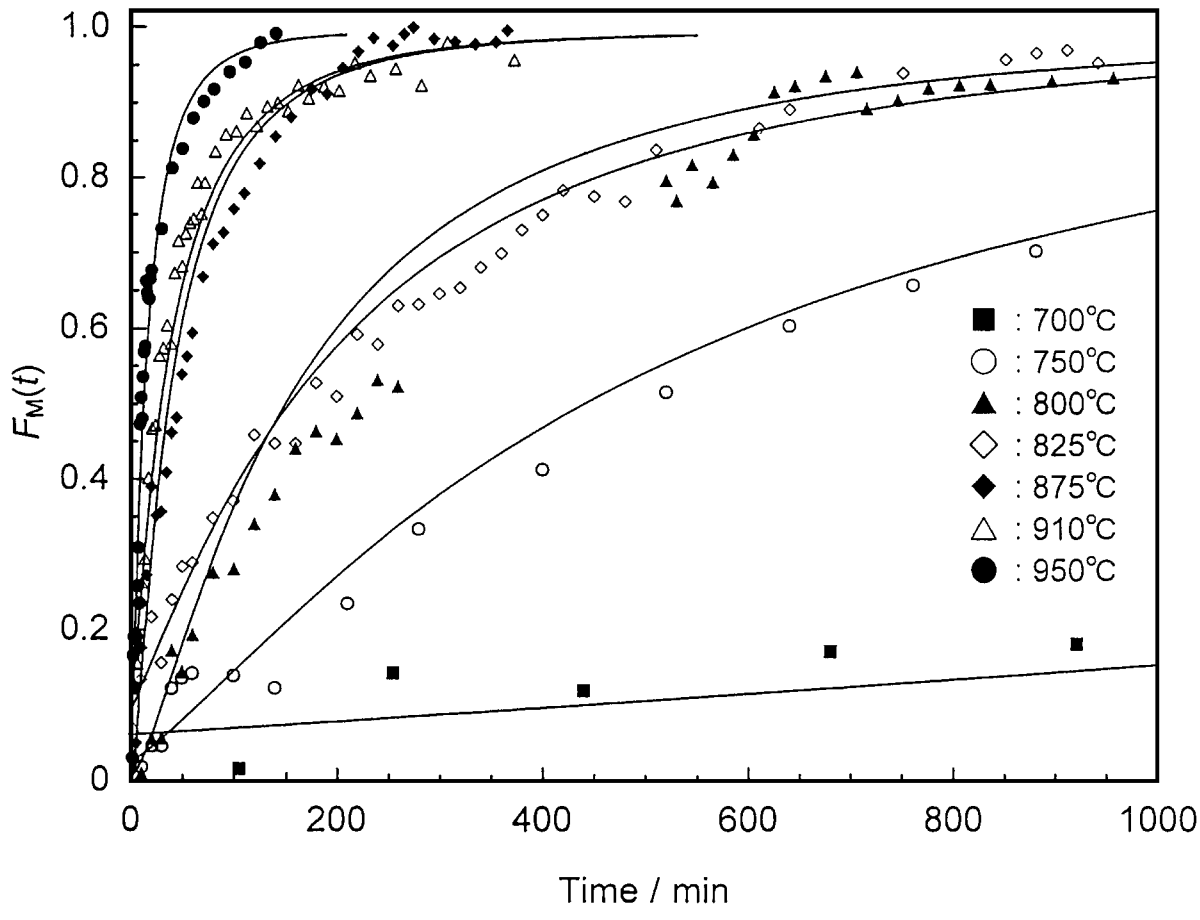

Figure 8 The results of $F_M(t)$ of Ohno's neutron diffraction as a function of $D_c'(0)$, $n\sigma$ and τ_n by Equation 18: (a) time range from 0 to 11500 min, (b) time range from 0 to 1000 min.

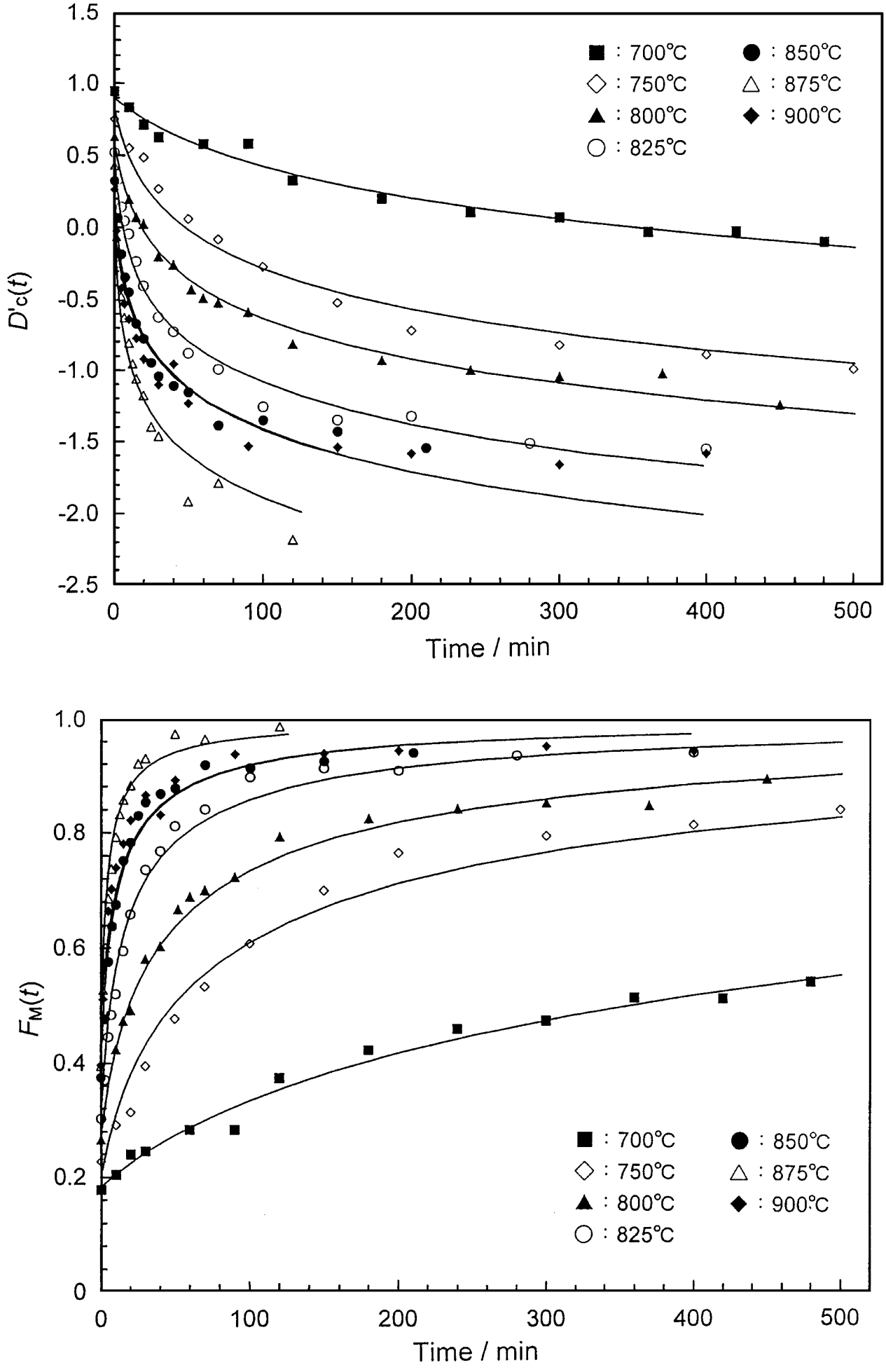

Figure 9 The results of (a) $D_c'(t)$ and (b) $F_M(t)$ of Ohno's X-ray diffraction as a function of $D_c'(0)$, $n\sigma$ and τ_n by Equation 18.

TABLE II Result of the Ohno's neutron experiment

$n\sigma = 1.06 \pm 0.03$

Temperature	$D_c'(0)$	τ_n
700 °C	1.54 ± 0.11	1344.7 ± 235.0
750 °C	1.95 ± 0.12	63.3 ± 12.1
800 °C	2.56 ± 0.31	10.6 ± 4.4
825 °C	1.33 ± 0.13	49.4 ± 9.8
875 °C	2.85 ± 0.66	1.9 ± 1.5
910 °C	1.41 ± 0.17	8.6 ± 2.1
950 °C	1.98 ± 0.22	1.8 ± 0.6

TABLE III Result of the Ohno's X-ray experiment

$n\sigma = 2.31 \pm 0.08$

Temperature	$D_c'(0)$	τ_n
700 °C	0.90 ± 0.07	50.3 ± 13.3
750 °C	0.85 ± 0.10	7.88 ± 2.45
800 °C	0.63 ± 0.11	5.73 ± 1.78
825 °C	0.60 ± 0.10	2.09 ± 0.65
850 °C	0.36 ± 0.11	1.70 ± 0.53
875 °C	0.50 ± 0.11	0.40 ± 0.13
900 °C	0.12 ± 0.09	2.94 ± 0.85

annealing temperature in the Ohno's experimental temperature range. The result of neutron experiment shows in Figs 7–8 and Table II and the X-ray experiment in Fig. 9 and Table III. As shown in these Figures, the fit of the neutron data is not as good as the fit of the X-ray data. Although we do not obtain the systematic temperature tendency of $D_c'(0)$ of Ohno's neutron diffraction, $D_c'(0)$ of Ohno's X-ray diffraction and τ_n of both Ohno's neutron and X-ray diffractions decrease with increasing the annealing temperature. $n\sigma$, $D_c'(0)$ and τ_n of neutron diffraction are very different from those of X-ray diffraction, respectively. A possible reason is that the sample volume of Ohno's neutron experiment was so large that all the samples were not the same temperature. Sample homogeneity and purity also possibly influence these discrepancies.

The values of τ_n in the present work are much larger than those of Ohno's experiment. Ohno suggested that the initial crystallite size is influenced by the phase-transformation rate. However, the crystallite size of the present work was almost the same as in Ohno's experiment. We believe that other factors related to the diffusion also probably affect the phase-transformation rate—for example, the shape of the crystallite and the amount of impurities.

4. Conclusions

We measured the transformation rates of the metastable tetragonal ZrO_2 to the monoclinic phase in air at 850–1000 °C by neutron diffraction. These rates increased with temperature. The phase transformation ended within 100 min at 1000 °C while it took more than 4000 min to complete at 850 °C. The transformation rates measured in our experiment were significantly lower then those measured by Whitney and Ohno et al.

The transformation kinetics can be understood by using our enhanced 'crystallite growth-martensitic transformation model', which includes the effects of the log-normal distribution of the crystallite size and normal grain-growth mechanism.

Acknowledgements

We are grateful to the staff of Solid State Division, ORNL, especially to Dr. H. R. Child for his constant encouragement and useful advice. We also wish to thank J. R. Weir, III, G. B. Taylor and R. G. Maples for their kindly assistance in the experiment. This work was carried out at ORNL under the U.S.-Japan Cooperative Program in Neutron Scattering. ORNL is managed by Lockeed Martin Energy Research Corporation under contracted DE-ACOS. 96 OR 22964 with the U.S. DOE.

References

1. D. J. GREEN, R. H. J. HAMINK and M. V. SWAIN, in "Transformation Toughening of Ceramics" (CRC Press Inc. Florida 1989) 5–15.
2. N. CLAUSSEN and M. RÜHLE, in "Advanced in Ceramics," Vol. 3, edited by A. H. Heuer, and L. W. Hobbs. (American Ceramic Society, Columbus, OH, 1981) 137–63.
3. T. SATO, S. OHTAKI and M. SHIMADA, *J. Mater. Sci.*, **20** (1985) 1466–70.
4. E. D. WHITNEY, *Trans Faraday Soc.*, **61** (1965) 1991–2000.
5. H. OHNO, Y. MORII, H. MURAKAMI, T. NAGASAKI, H. KATSUTA, M. IIZUMI, H. R. CHILD and R. M. NICKLOW, *JAERI-M*(1987) 60–78.
6. M. AVRAMI, *J. Chem. Physics*, **7** (1939) 1103–12: **8** (1940) 212–24: **9** (1941) 177–84.
7. H. MURAKAMI and H. OHNO, *Nippon Ceramic Kyokai Gakujutsu Ronbunshi*, **99** (1991) 1224–1239.
8. R. C. GARVIE, *J. Phys. Chem.*, **69** (1965) 1238–43: **82** (1978) 218–24.
9. N. IGAWA, Y. ISHII, T. NAGASAKI, Y. MORII, S. FUNAHASHI and H. OHNO, *J. Am. Ceram. Soc.*, **76** (1993) 2673–76.
10. S. KATANO, H. MOTOHASHI and M. IIZUMI, *Rev. Sci. Instrum.*, **57** (1986) 1409–1412.
11. R. J. BROOK, in "*Treatise on Materials Science and Technology*," Vol. 9, edited by F. Wang. (Academic Press, NY, 1976). 331–64.
12. S. K. KURTZ and F. M. A. CARPAY, *J. Appl. Phys.*, **51** (1980) 5725–44.
13. *Idem.*, *ibid.*, **51** (1980) 5745–54.

Received 16 March
and accepted 15 July 1998